Journal of Medicinal Chemistry

Article

pubs.acs.org/jmc

Wnt Inhibition Correlates with Human Embryonic Stem Cell Cardiomyogenesis: A Structure−Activity Relationship Study Based on Inhibitors for the Wnt Response

Marion Lanier,*[†,§,∥] Dennis Schade,[†,‡,§,∥] Erik Willems,[‡,§] Masanao Tsuda,[‡] Sean Spiering,[‡] Jaroslaw Kalisiak,[†] Mark Mercola,[‡,§] and John R. Cashman[†,§]

[†]Human BioMolecular Research Institute, 5310 Eastgate Mall, San Diego, California 92121-2804, United States

[‡]Sanford−Burnham Medical Research Institute, 10901 North Torrey Pines Road, La Jolla, California 92037, United States

[§]ChemRegen Inc., 11171 Corte Cangrejo, San Diego, California 92130, United States

Supporting Information

ABSTRACT: Human embryonic stem cell-based high-content screening of 550 known signal transduction modulators showed that one "lead" (**1**, a recently described inhibitor of the proteolytic degradation of Axin) stimulated cardiomyogenesis. Because Axin controls canonical Wnt signaling, we conducted an investigation to determine whether the cardiogenic activity of **1** is Wnt-dependent, and we developed a structure−activity relationship to optimize the cardiogenic properties of **1**. We prepared analogues with a range of potencies (low nanomolar to inactive) for Wnt/β-catenin inhibition and for cardiogenic induction. Both functional activities correlated positively (r^2 = 0.72). The optimal compounds induced cardiogenesis 1.5-fold greater than **1** at 30-fold lower concentrations. In contrast, no correlation was observed for cardiogenesis and modulation of transforming growth factor β (TGFβ)/Smad signaling that prominently influences cardiogenesis. Taken together, these data show that Wnt signaling inhibition is essential for cardiogenic activity and that the pathway can be targeted for the design of druglike cardiogenic molecules.

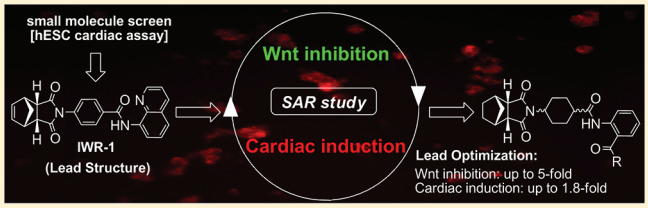

INTRODUCTION

The proposal to produce human heart muscle cells from stem cells has attracted much attention because of the potential for promising applications in medicine and drug discovery, ranging from cell transplantation to in vitro pharmacological testing. Use of human stem cell-derived cardiomyocytes as tools for drug discovery and development (i.e., high-throughput assays, specific disease models, target identification and validation, or toxicity assessment) has many advantages over current assays that rely on a noncardiomyocyte setup.[1−3] Cardiomyocytes, the key cells for cardiac safety evaluation at the preclinical stage, are hard to come by. Scientists are usually limited to animal-derived cells or tissues or human engineered cells (cell lines heterologously expressing human cardiac ion channels, cardiac cell cultures, isolated tissue preparations, and perfused animal hearts) that have limited predictivity in humans. For example, overexpression of the hERG channel in fibroblasts is commonly used in drug development as a model to evaluate cardiotoxicity of novel drugs. One major advantage of cardiomyocytes derived from human embryonic stem cells is that they are of human origin and can be maintained in culture for extended time periods without losing their characteristics. Theoretically, they represent an unlimited source for human cardiomyocytes for in vitro testing. Moreover, the information gained from developing small molecules for stem cell-derived cardiomyocyte differentiation in vitro may lead to the development of drugs capable of mobilizing endogenous cardiac progenitor cells to regenerate damaged muscle in the adult heart.[4]

Cell differentiation is a complex and still poorly understood process. As for other tissue types, the development of human myocardial cells requires close temporal control of inducing factors to stimulate the stepwise progression from pluripotent cells to uncommitted progenitor to committed precursor and finally to myocardial cells including cardiomyocytes.[4,5] Current approaches to stimulate stem cell differentiation have included naturally occurring factors, the introduction of lentiviral vectors carrying transcription factors, the addition of growth factors, and the use of small-molecule signaling pathway modulators.[1] The approach described herein focuses on the latter, because use of small molecules as differentiation reagents overcomes the inherent high cost of biological factors or reagents for in vitro applications, and they can be developed into drug candidates for in vivo applications for therapeutic development.

We recently described a human embryonic stem cell (hESC)-based high-content screen (HCS) of about 550 known pathway modulators (i.e., InhibitorSelect and StemSelect, both from EMD Chemicals Inc.) and used these compounds to identify key signaling pathway(s) that control differentiation of uncommitted cardiac progenitors to form cardiomyocytes.[6]

Received: July 30, 2011
Published: December 22, 2011

Only one small molecule [**1** (IWR-1),[7,8] Figure 1] was identified as a "lead" from this library screen. The abbreviation

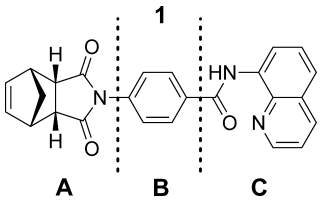

Figure 1. Screening "lead" **1**. Regions A, B, and C indicate the different areas of the molecule that were systematically modified for lead optimization.

IWR stands for Inhibitor of the Wnt Response. Wnt is a hybrid name of Int, a gene active in mouse mammary tumors, and Wingless, a gene essential for wing development in *Drosophila*. The Wnt pathway has been studied in a wide range of organisms and is implicated in mammalian development and cancer. Compound **1** was recently reported as an inhibitor of the oncogenic canonical Wnt response at the Axin level.[7,8] Besides being involved in cancer,[9] Wnt and Wnt inhibition regulate crucial processes during embryonic development.[10] Wnt signaling plays a multiphasic role in heart development, and Wnt inhibition is critical to form committed progenitor cells.[11,12] This has led to the use of the natural Wnt inhibitor Dickkopf-1 (DKK-1) to enhance cardiogenesis in hESC culture[13] and the discovery of small-molecule tool compounds.[2]

Herein, we examined the effect of the previously reported Wnt inhibitors **1**−**5** (Figure 2A) on human ESC-mediated cardiomyocyte differentiation in parallel with a stepwise process to improve the pharmacological properties of **1**. Compound **1** was optimized for its ability to inhibit the Wnt pathway and stimulate cardiogenesis. Newly designed compounds **10**, **29**, and **34** showed decreased IC_{50} values for inhibition of the Wnt pathway as well as increased cardiomyogenesis potency. Compared to **1**, compounds **10**, **29**, and **34** showed improved functional activity and improved physiochemical properties, thus rendering them more attractive for in vitro and possibly in vivo studies.

■ CHEMICAL SYNTHESIS

The synthesis of **1** and certain analogues was recently described in papers reporting new Wnt inhibitors for cancer.[7,8] From a structural perspective and as previously described by Lu et al.,[8] compound **1** can be divided into three regions (A, B, and C in Figure 1). The structure−activity relationships (SAR) of all three regions of **1** were explored.

Regions A and C were modified via synthetic protocols described by Chen et al.,[7] (Schemes 1 and 2). Briefly, the desired amino acid **6** was heated with anhydride **7** in *N*,*N*-dimethylformamide (DMF) and afforded intermediates **8a**−**e** in good yields. The carboxylic acid moiety of **8a**−**e** was then activated in the presence of thionyl chloride and treated with the appropriate amine (R_3NH_2) to give compounds **9**−**39** and **53**−**56** (Scheme 1). Compounds **41**, **42c**−**f**, **43g**−**k**, and **44l**−**p** were prepared by treating the acid chloride of *p*-nitrobenzoic acid with the appropriate amine, R_3NH_2. After hydrogenation of the nitro group, intermediate **40** was subjected to a reductive amination step or acylation or treatment with an anhydride to give the desired products **41**−**44** (Scheme 2).

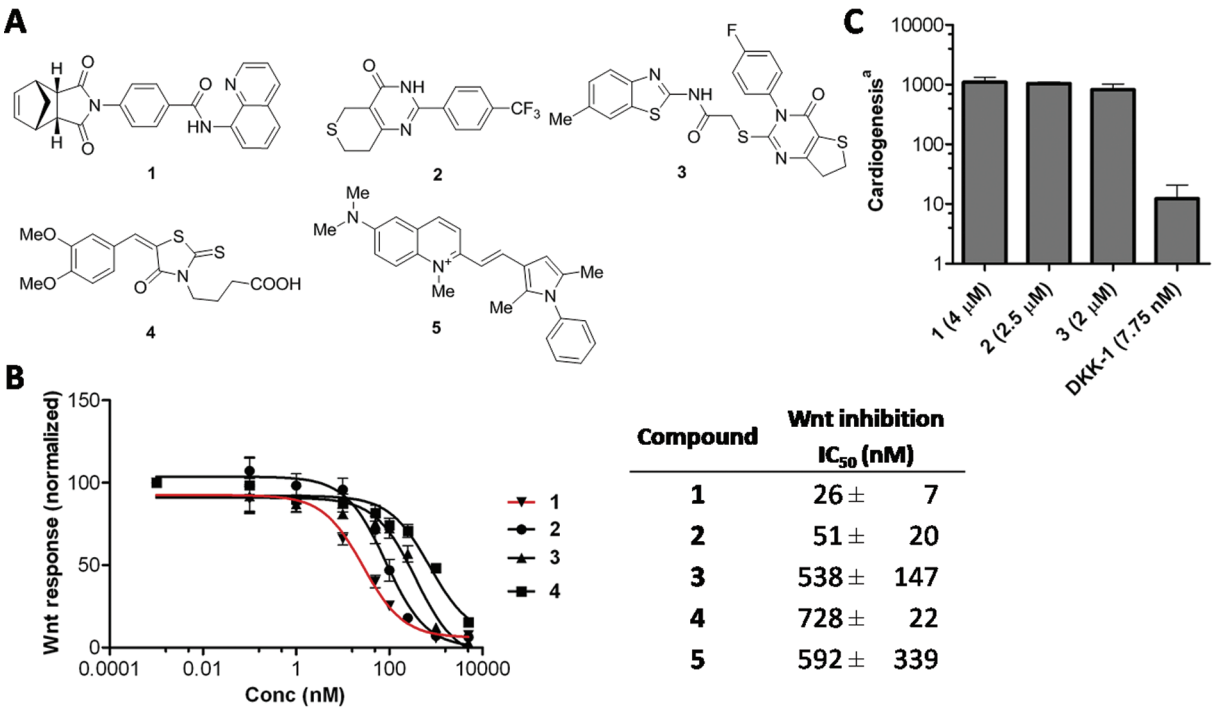

Compound	Wnt inhibition IC_{50} (nM)
1	26 ± 7
2	51 ± 20
3	538 ± 147
4	728 ± 22
5	592 ± 339

Figure 2. Inhibition of the Wnt pathway with reported inhibitors **1**−**5**. (A) Structures of compounds **1**−**5**. (B) Dose−response curves and IC_{50} values for Wnt inhibition for **1**−**5**, representing different classes of Wnt inhibitors. Data is the mean ± standard deviation of at least three independent experiments. (C) Maximum cardiogenesis in the presence of Wnt inhibitors in hESCs (data from Willems et al.);[6] human recombinant DKK-1 = 200 ng/mL (7.75 nM). [a] Cardiogenesis corresponds to MYH6-mCherry expression levels as fold induction over DMSO vehicle control (=1-fold).

Scheme 1. Synthesis of Analogues 9−39 and 53−56[a]

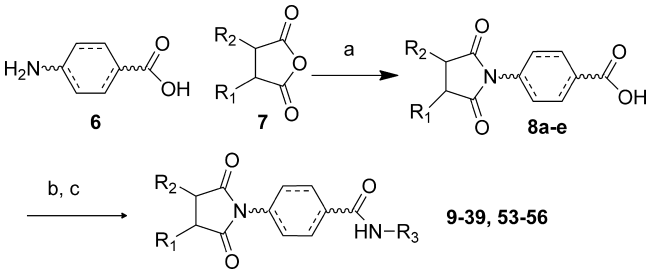

[a](a) DMF, 120 °C, 16 h. (b) Thionyl chloride, DMF, 80 °C, 16 h. (c) R_3NH_2, Py, DCE, room temp to 50 °C, 16 h.

The SAR of region B was explored by various synthetic approaches. Compound **45** (Table 1) was prepared following the same sequence of steps as in Scheme 1 but with **6** replaced by 3-aminobenzoic acid. Compound **46** (Table 1) was prepared following Scheme 2 with 4-nitrobenzoic acid replaced by 5-nitro-2-furoic acid. Compound **48** was prepared in three steps from 4-nitrophthalic anhydride (Scheme 3). Condensation of 5-nitroisobenzofuran-1,3-dione with 8-aminoquinoline followed by reduction of the nitro group afforded **47**. Condensation of **47** with *cis*−*endo*-dihydrocarbic anhydride under conditions described in Scheme 1 afforded **48**. For the reduced version **50** (Table 1), intermediate **49** was obtained in two steps by reductive amination of 8-aminoquinoline with 4-nitrobenzaldehyde followed by reduction of the nitro group with sodium dithionite. Compound **49** was treated with *cis*−*endo*-dihydrocarbic anhydride under conditions described in Scheme 1 to afford compound **50** (Scheme 4). Finally, the reverse amide **52** (Table 1) was synthesized via intermediate **51**. Treatment of 4-nitroaniline with carbic anhydride followed by hydrogenation gave **51**, and following addition of freshly prepared quinoline-8-carbonyl chloride, treatment with aniline provided the desired reverse amide (**52**, Scheme 5).

Table 1. SAR for Central Region B of the Molecule for Wnt Inhibition

	Cpd#	% inhibition (1 μM)	IC_{50} (nM)
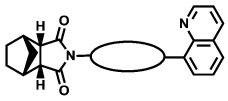			
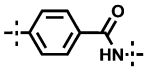	**9**	93 ± 1	24 ± 4
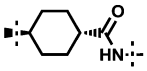	**10**	89 ± 2	4 ± 2
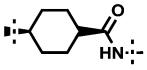	**11**	90 ± 1.4	57 ± 5
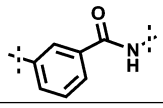	**45**	0	NM[a]
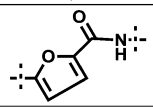	**46**	0	NM
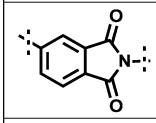	**48**	15 ± 2	NM
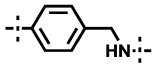	**50**	45 ± 3	NM
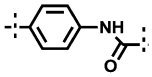	**52**	91 ± 1	119 ± 9

[a]NM, not measured.

RESULTS AND DISCUSSION

Because **1**, the lead compound from screening, was reported to inhibit canonical Wnt signaling at the Axin level,[7] we compared **1** to four mechanistically different Wnt inhibitors [**2** (XAV939),

Scheme 2. Synthesis of Compounds 41−44[a]

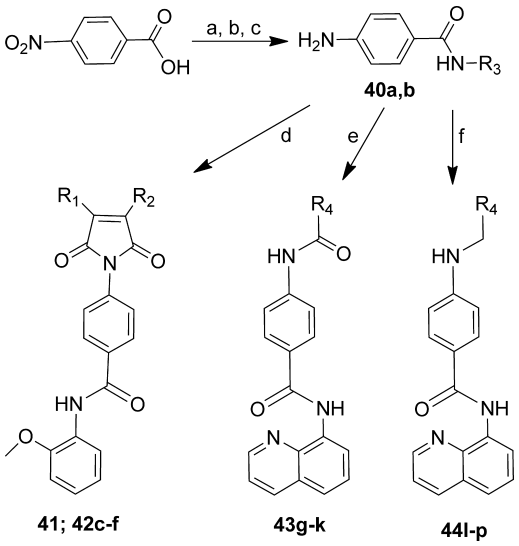

40a: R_3=2-methoxyphenyl
40b: R_3=quinolin-8-yl
41: R_1,R_2 form a cyclohexyl
42c: R_1,R_2=Cl
42d: R_1=Cl, R_2=dimethylamine
42e: R_1=Cl, R_2=cyclobutyl
42f: R_1=Cl, R_2=i-butyl
43g: R_4=cyclohexyl
43h: R_4=t-butyl
43i: R_4= m-tolyl
43j: R_4= o-tolyl
43k: R_4= noradamantyl
44l: R_4= isobutyl
44m: R_4=cyclopropyl
44n: R_4=cyclohexyl
44o: R_4=o-CF_3-phenyl
44p: R_4=5-F-2-OMe-phenyl

[a](a) Thionyl chloride, reflux, 2 h. (b) R_3NH_2, pyridine, reflux, 3 h. (c) H_2, Pd/C, EtOH, room temp, 16 h. (d) Anhydride, TEA, DMF, 120 °C, 16 h. (e) R_4COCl, TEA, DCE, 70 °C, 16 h. (f) R_4CHO, $NaBH(OAc)_3$, AcOH, $MgSO_4$, DCE, 50 °C, 72 h.

Scheme 3. Synthesis of 48[a]

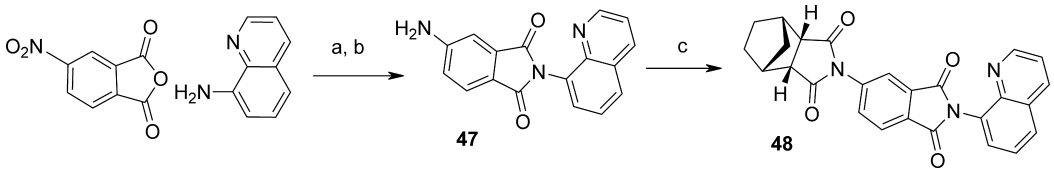

[a](a) DMF, 120 °C, overnight. (b) H_2, Pd/C, EtOH, room temp, overnight. (c) *cis*-Endodihydrocarbic anhydride, DMF, 120 °C, 10 h.

Scheme 4. Synthesis of 50[a]

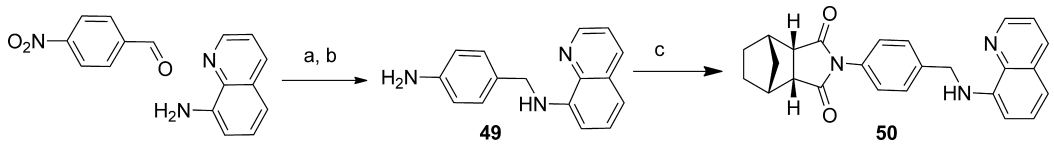

[a](a)$NaBH_3CN$, AcOH, EtOH, room temp, 16 h. (b) $Na_2S_2O_4$, EtOH/$NaHCO_3$aqueous, room temp, 16 h. (c) *cis*-Endodihydrocarbic anhydride, DMF, 120 °C, 16 h.

Scheme 5. Synthesis of 52[a]

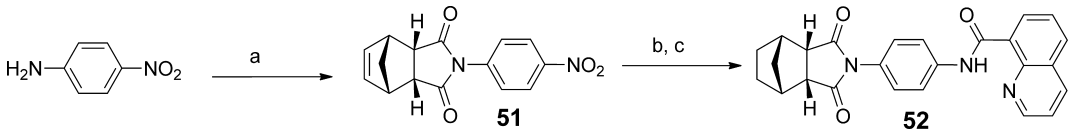

[a](a) *cis*-Endocarbic anhydride, DMF, 120 °C, 16 h. (b) H_2, Pd/C, EtOH, room temp. (c) Quinoline-8-carbonyl chloride, TEA, 3 days, room temp.

3 (IWP-3), **4** (iCRT-5), and **5** (pyrvinium); Figure 2A] in a Wnt inhibition assay (Figure 2B) and a hESC cardiogenesis assay (Figure 2C) to examine the relation between Wnt inhibition and cardiogenesis and to narrow down and identify the part of the pathway blocked in the signaling cascade that influenced cardiogenic activity. To ensure that the SAR analysis was not confounded by cell toxicity, the five Wnt inhibitors (**1**−**5**) and certain analogues of **1** were tested in parallel for cytotoxicity (see Supporting Information, Figure S2). Compound **1** blocks the Wnt pathway by stabilizing the Axin protein complex via a direct interaction with Axin.[7] Compound **2** stabilizes Axin by inhibiting the poly-ADP-ribosylating enzymes tankyrase 1 and 2.[14] Compound **3** inhibits the production of Wnt by preventing the palmitoylation of Wnt proteins by Porcupine.[7] Compound **4** has been reported to inhibit the interaction between β-catenin and TCF4 within the cell nucleus.[15] Compound **5** activates CK1α activation in the Wnt pathway and promotes degradation of β-catenin and inhibited Axin degradation.[16] In our hands, **5** was a very modest Wnt inhibitor (IC_{50} = 592 nM) and also quite cytotoxic, so it was not tested in the cardiac assay. Compounds **3** and **4** were similarly modest Wnt inhibitors (i.e., IC_{50} = 538 and 728 nM, respectively) but were not toxic to HEK293T cells at concentrations up to 20 μM (see Figure S2 in Supporting Information). Compound **2**, described to induce cardiac differentiation in mouse ESCs,[17] had an IC_{50} of 51 nM in the Wnt assay and did not induce cell toxicity. Compound **1** had a similar profile (i.e., IC_{50} = 26 nM and was not toxic to HEK293T cells). As we showed previously,[6] **1**, **2**, and **3** induced cardiogenesis by ca. 1000-fold at their maximum efficacious concentrations (i.e., 4, 2, and 2.5 μM respectively; Figure 2C) over a dimethyl sulfoxide (DMSO) control but differed in their potencies. Compound **2** was about 1.5-fold less potent than **1** and **3**. Compound **4** was weakly cardiogenic but only at a higher concentration (50 μM). Compound **3** was not selected as a lead candidate because its mode-of-action in inhibiting Wnt production is reported to be at an upstream position compared to **1**. Taken together, these data suggested that **1** was the most appealing structure as a lead candidate. It was potent both as a Wnt inhibitor and as a cardiogenic agent in the hESC studies and was not cytotoxic to the cells examined.

Wnt Inhibition. Initially, a structurally diverse library of ca. 90 analogues of **1** was synthesized and tested for Wnt inhibition at a standard concentration (i.e., 1 μM). Compounds that showed inhibition above 50% at 1 μM were re-evaluated for dose-dependent inhibition. Next, more focused libraries were prepared to improve potency and physicochemical features of promising analogues.

By use of synthetic strategies depicted in Schemes 1−5, variations on the central region (region B) were prepared and evaluated for Wnt inhibition (Table 1). Lu et al.[8] previously showed that the phenyl ring of **1** could be replaced by a *trans*-cyclohexyl moiety and still maintain Wnt inhibition potency. As shown in Table 1, an increase in Wnt inhibition potency was observed with the completely saturated *trans*-cyclohexyl analogue **10** (IC_{50} = 4 nM). Because a cyclohexyl ring can adopt both cis and trans configurations, it was of interest to examine the stereoselectivity of Wnt inhibition. The cis analogue **11** was prepared and found to be potent (i.e., IC_{50} = 57 nM). It is possible that the potency of the *cis*-cyclohexyl moiety can be explained by **11** adopting a boat conformation. Next, modifications of the amide function revealed important information about Wnt inhibition SAR. Reducing the amide function (**50**, 45% inhibition at 1 μM), changing the amide position to the meta position (**45**, 0% inhibition at 1 μM), or replacing the central aryl substituent by a furan group (**46**, 0% inhibition at 1 μM) decreased the potency of Wnt inhibition and showed that both the amide bond and the 1,4-substitution pattern for the central B region were essential for maximal

inhibitory potency. A rigidified version (**48**) and a reverse-amide version (**52**) were also prepared. Reversing the amide as in **52** was tolerated but showed some loss of Wnt inhibitory potency (IC_{50} = 119 nM), while the rigid analogue **48** was inactive (15% inhibition at 1 μM). Compounds **9** (central phenyl ring) and **10** (central *trans*-cyclohexyl ring) possessed similar IC_{50} values (24 and 4 nM, respectively), which suggested that the central ring itself likely seems to be a simple placeholder and does not contribute to a discernible biological interaction.

A systematic study of the effect of position of the nitrogen atom in the quinoline heterocycle on Wnt inhibition was done with compounds possessing a *trans*-cyclohexyl ring in the central position. The results summarized in Tables 2 and 3 show that the 8-aminoquinoline isomer was the most potent quinoline (**10**, IC_{50} = 4 nM). Potency decreased when the distance between the quinoline nitrogen and the amide function increased, suggesting either an intramolecular interaction between the amide hydrogen and the quinoline nitrogen or, alternatively, a specific interaction with a biological target. Lu et al.[8] showed that replacement of the quinoline with a phenyl ring substituted at various positions by halogens or a trifluoromethyl group usually led to a significant loss of potency. The optimal aryl substitution pattern was for a 4-bromophenyl and 2-methoxyphenyl (IC_{50} = 100 nM for both compared to 200 nM for **1**).[8] Incorporation of electron-donating groups (2-hydroxyl compound **19**, 33% inhibition at 1 μM; 2- and 4-methoxy compounds **20** and **21**, 50% inhibition at 1 μM and IC_{50} = 215 nM; 4-dimethylamino compound **22**, 25% inhibition at 1 μM) or electron-withdrawing groups (4-cyano compound **23**, IC_{50} = 317 nM; 4-acetyl compound **24**, 41% inhibition at 1 μM) did not lead to a clear picture of the effect of electronic substituents on Wnt inhibition (Table 3). On the other end, the presence of a methoxy group at the ortho position (compound **21**, IC_{50} = 215 nM) or a *p*-methoxy substituent (**22**, 50% inhibition at 1 μM) suggested that the electronic nature of the substituent at the aryl ring was not critical for Wnt inhibition. It is likely that shape rather than electronic properties and the position of the substituent affected potency. A carbonyl-containing functionality at the ortho position afforded the most potent analogues examined and apparently mimicked the role of the quinoline nitrogen to afford potent Wnt inhibition. A methyl ester at the 2-position (**27**) had an IC_{50} of 67 nM, and the 2-methylketone (**28**) had an IC_{50} of 6 nM. The tetralone analogue **29** was similarly potent (IC_{50} = 7 nM). When increased steric bulk was introduced by 9*H*-fluoren-9-one (**30**, IC_{50} = 194 nM), potency decreased, suggesting steric hindrance in this region may have a negative effect on Wnt inhibition (Table 3).

Table 2. SAR for Region C: Systematic Study of the Effect of Nitrogen Position of the Quinoline Heterocycle on Potency for Wnt Inhibition

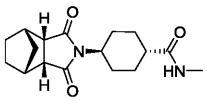	Cpd #	% inhibition (1 μM)	IC_{50} (nM)
Naphtalen-1-yl[a]	**12**	41 ± 13	1590 ± 280
isoquinolin-1-yl	**13**	88 ± 1	95 ± 3
isoquinolin-4-yl	**14**	89 ± 2	55 ± 8
quinolin-4-yl	**15**	90 ± 1	109 ± 7
quinolin-4-yl	**16**	68 ± 4	604 ± 90
isoquinolin-5-yl	**17**	87 ± 1	161 ± 16
isoquinolin-8-yl	**18**	91 ± 1	93 ± 4
quinolin-8-yl	**10**	89 ± 2	4 ± 2

[a]Compound **12** has a phenyl central ring instead of the *trans*-cylcohexyl.

A number of unsubstituted heterocycles [2-pyrimidine, 2-pyrazine, 3-(1,2,4-triazole), 2-thiazole, 2-pyridine, 3-pyridine, and 4-pyridine] were synthesized as replacements for the quinoline substituent. While the unsubstituted 2-, 3- and 4-pyridines (compounds **31**−**33**, Table 3) showed IC_{50} values in the 100 nM range (IC_{50} = 109, 120, and 80 nM, respectively), none of the other heterocycles described above were functionally active (inhibition below 50% at 1 μM; data not shown). Substituted pyridines were then prepared by combining the optimal substituents identified from the data of Table 3 with 3- and 4-pyridine derivatives. Compounds combining the 3-pyridine with an acetyl group at the 2- or 6-position were prepared and tested. Remarkably, the 2-acetyl-3-pyridine analogue **34** gave an IC_{50} value of 7 nM, while the 6-acetyl-3-pyridine isomer **35** was significantly less potent (IC_{50} = 590 nM).

As reported (but not exemplified) by Lu et al.,[8] region A (Figure 1) was very sensitive to chemical modifications. In our hands, any attempts to modify this region, either by replacing the bicycle by bulky R groups (i.e., compounds **41** and **42c**−**f**, Scheme 2) or replacing the entire carbic moiety by various groups (compounds **43g**−**k** and **44l**−**p**, Scheme 2), led to a complete loss of potency (inhibition < 32% at 1 μM). Only minor structural alterations such as saturation of the double bond (**9**, IC_{50} = 24 nM) were well-tolerated; two-carbon-bridge analogues (**36**, IC_{50} = 412 nM, and **37**, IC_{50} = 314 nM; Table 4) and oxa analogue (**39**, IC_{50} = 605 nM) were >10-fold less potent. Adding a methyl group to the carbic moiety (**38**, IC_{50} =1176 nM) also resulted in significant loss of potency, highlighting the sensitivity of this region to substitution.

Chemical Stability. Certain selected compounds, as well as **1** for comparison purposes, were evaluated for chemical stability in buffer before being tested for their cardiogenic properties. hESC cardiogenesis studies were done in a cell-based assay at pH 7.4, and biological activity was presumably required for at least 24 h after compound addition, 4 days after initiating hESC differentiation.[6] Therefore, we determined the aqueous stability of key compounds at pH 7.4 for at least 24 h. Representatives of the various subseries, (compounds **1**, **10**, **28**, **32**, and **52**), were incubated at 10 μM in phosphate buffer (pH 7.4) for up to 30 h. No degradation was observed as determine by HPLC for any of the compounds except **52**, whose half-life was 3.8 h (Supporting Information, Table S1).

Induction of Cardiogenesis. From the 180 synthetic analogues tested in the Wnt inhibition assay, 26 were selected to examine cardiogenic induction in the presence of hESCs. This subset of analogues comprised a full range of inhibitory potency in the Wnt assay and contained the most structurally diverse scaffolds for evaluation of hESC cardiogenic activity. As shown in Figure 3, analogues from the following series were selected as representative members to investigate (a) variation of the N-position of the quinoline C region, including phenyl

Table 3. SAR of Region A: Effects of Phenyl and Pyridinyl Substituents on Potency for Wnt Inhibition

		Cpd #	% inhibition (1 μM)	IC_{50} (nM)
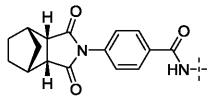	2-hydroxy-phenyl	**19**	33 ± 5	NM[a]
	4-methoxy-phenyl	**20**	50 ± 2	NM
	2-methoxy-phenyl	**21**	84 ± 2	215 ± 18
	4-dimethylamino-phenyl	**22**	25 ± 25	NM
	4-cyano-phenyl	**23**	70 ± 2	317 ± 8
	4-acetylphenyl	**24**	41 ± 13	NM
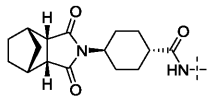	2-hydroxy-phenyl	**25**	76 ± 3	484 ± 196
	2-ethoxyphenyl	**26**	78 ± 2	190 ± 46
	2-CO_2Me-phenyl	**27**	86 ± 16	67 ± 10
	2-COMe-phenyl	**28**	91 ± 1	6 ± 3
	8-oxo-5,6,7,8-tetrahydronaphthalen-1-yl	**29**	92 ± 13	7 ± 1
	(9*H*-fluorene-9-one)-1-yl	**30**	88 ± 2	194 ± 20
	2-pyridinyl	**31**	82 ± 5	109 ± 4
	3-pyridinyl	**32**	89 ± 1	120 ± 32
	4- pyridinyl	**33**	84 ± 1	80 ± 10
	2-acetyl-3-pyridinyl	**34**	79 ± 1	7 ± 2
	6-acetyl-3-pyridinyl	**35**	56 ± 3	590 ± 153
	2-methoxy-4-bromophenyl	**53**	82 ± 5	37 ± 12
	5-hydroxy-pyridin-3-yl	**54**	86 ± 2	152 ± 25
	2-chloro-pyridin-3-yl	**55**	13 ± 1	169 ± 45
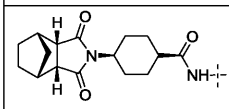	2-COMe-phenyl	**56**	91 ± 1	23 ± 5

[a]NM, not measured.

Table 4. SAR for Region A of the Molecule for Wnt Inhibition

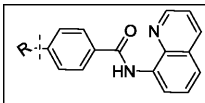	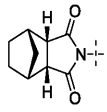	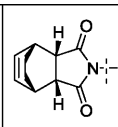	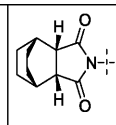	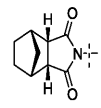	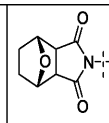
Cpd #	**9**	**36**	**37**	**38**	**39**
%inh (1 μM)	93 ± 1	83 ± 4	87 ± 1	76 ± 1	49 ± 4
IC_{50} (nM)	24 ± 4	412 ± 26	314 ± 19	1176 ± 260	605 ± 260

versus pyridinyl substituents and *o*-carbonyl groups; (b) variation of the central B region linker, including aromatic versus aliphatic and cis- versus trans-configured linkers; and (c) variation in the norbornene A region moiety. Figure 3A shows a list of values for the potency of Wnt inhibition in HEK293T cells and induction of cardiogenesis in hESCs. Three classes of compounds stimulated hESC cardiogenesis. The first group of compounds (**32**, **21**, **35**, **33**, **31**, **39**, **37**, **23**, **52**, and **12**) was

A

Compd	hESC Cardiogenesis % Cardiogenesis[a]	hESC Cardiogenesis Z Score[b]	Wnt Inhibition IC_{50} (nM)
29	176 ± 86	108 ± 5	4 ± 1
34	145 ± 112	74 ± 12	2 ± 1
10	136 ± 48	133 ± 74	4 ± 2
14	119 ± 36	22 ± 19	55 ± 8
30	104 ± 43	94 ± 51	194 ± 20
1	100 ± 27	13 ± 6	26 ± 7
13	84 ± 14	3 ± 1	95 ± 3
28	75 ± 28	62 ± 35	6 ± 3
56	72 ± 34	18 ± 1	23 ± 5
9	68 ± 17	10 ± 7	24 ± 4
11	65 ± 12	48 ± 17	57 ± 5
54	61 ± 15	16 ± 7	152 ± 25
55	56 ± 31	1 ± 1	169 ± 45
27	38 ± 31	21 ± 3	67 ± 10
18	25 ± 12	0	93 ± 4
53	20 ± 5	8 ± 4	37 ± 2
32	15 ± 2	2 ± 1	120 ± 32
21	8 ± 2	2 ± 1	215 ± 18
35	3 ± 1	0	590 ± 153
33	3 ± 1	0	80 ± 1
31	3 ± 2	1 ± 1	109 ± 4
39	2 ± 1	0	605 ± 260
37	2 ± 1	1 ± 1	314 ± 19
23	1 ± 1	0	317 ± 8
52	1 ± 1	0	119 ± 9
12	0	0	1590 ± 280

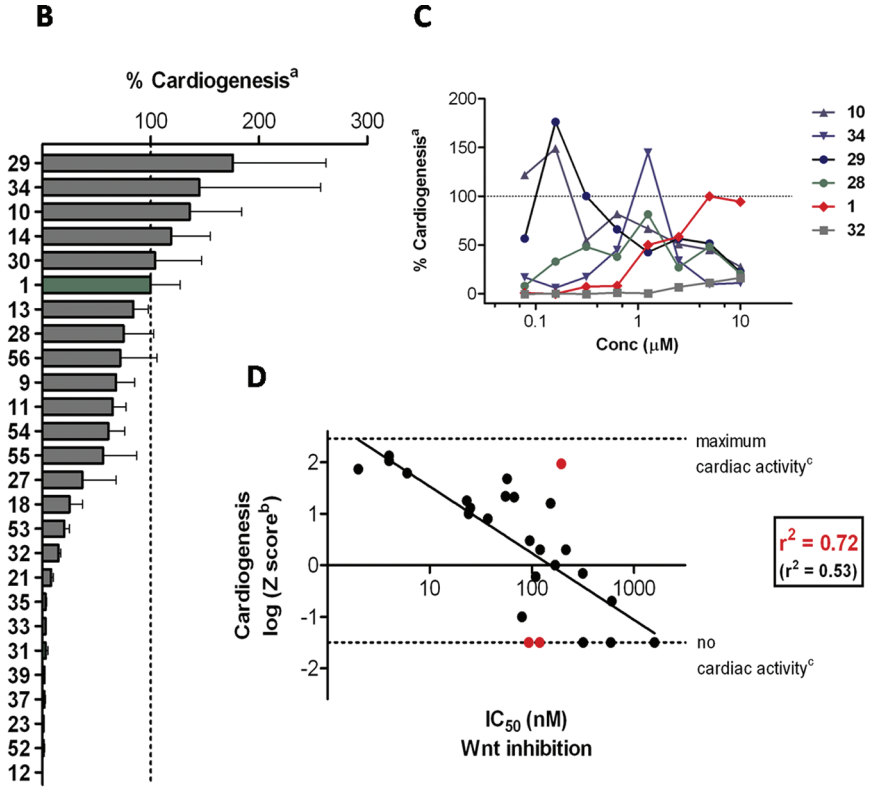

Figure 3. Cardiogenic activity and Wnt inhibition of selected analogues. (A) Data set for analogues tested in cardiac and Wnt assays; IC_{50} values (nanomolar) were measured in the Wnt inhibition assay. Those highlighted in red are outlier compounds. (B) Maximum cardiogenic activity for each compound tested relative to the maximum induction for **1** (set at 100%). (C) Representative dose−response curves of IWR analogues in hESCs for cardiogenesis. (D) Correlation of cardiogenesis (based on the *Z*-score at 625 nM) and Wnt inhibition (IC_{50} values) in a double-logarithmic plot; data points (in red) indicate outlier derivatives that were excluded from the correlation (this r^2 is highlighted in red). The correlation coefficient r^2 shown in black includes all data. [a] Percent cardiogenesis represents normalized data for most effective (cardiac) concentration to the maximum induction of **1** (100% at 2.5 μM). [b] *Z*-score at a dose of 625 nM. [c]Maximum cardiac activity = normalized to **1**, no cardiac activity = *Z*-score of ≤0.

functionally inactive as inducers of cardiogenesis and possessed uniformly large IC_{50} values in the Wnt inhibition assay (>200 nM). A subset of these compounds (**31**, **32**, and **33**), however, had IC_{50} values in the 100 nM range as Wnt inhibitors. Further studies need to be done to explain their biological properties. Compound **52** contained a "reverse amide" and was a relatively potent Wnt inhibitor (IC_{50} = 119 nM) but was inactive as a cardiogenic inducer. The chemical half-life of **52** has been estimated to be less than 5 h in the presence of assay buffer (see Supporting Information, Table S1) and this could explain its low cardiogenesis functional activity. While lack of aqueous stability would not be expected to compromise functional activity in the short time frame of the Wnt assay, the actual concentration of **52** in the hESC assay may have declined compared to the time necessary to induce cardiogenesis and thus could explain its lack of potency as a cardiogenic stimulant. The second class (**14**, **30**, **1**, **13**, **56**, **9**, **11**, **55**, **54**, **27**, **18**, and **53**) contained compounds that elicited a dose-dependent induction of cardiogenesis functional activity, without a decrease in cardiogenesis at higher doses. These compounds were also potent Wnt inhibitors on the basis of their IC_{50} values in the Wnt assay (20−200 nM). Compound **30** exhibited modest Wnt inhibition (IC_{50} = 194 nM) and solid cardiac induction (104% cardiogenesis). We suspect that the high lipophilicity of the 9-fluorene substituent causes low aqueous solubility and extensive protein binding. This could possibly explain the observed differences in these two distinct assays. The third class of compounds (**29**, **34**, **10**, and **28**) were potent Wnt inhibitors and potent stimulators of cardiogenesis, even at low concentrations (i.e., < 0.15 μM). They were distinguishable from the second group of compounds by their dose−response curves (Figure 3C). They showed very strong cardiogenesis at the lowest concentrations, followed by a constant decrease of percent cardiogenesis at increasing compound concentration in the cell-based assay. This effect could be due to anticardiogenic, antiproliferative, or toxic cellular effects caused by strong Wnt inhibition. Compared to other analogues, compound **52** was substantially less stable at pH 7.4 than other analogues (see Supporting Information, Table S1) and thus its potency in the hESC assay may be possibly underestimated. Compound **18** had a negative *Z*-score at 625 nM and thus appeared as an outlier in our correlation, but it was cardiogenic at higher concentrations and reached 24% maximum cardiogenesis at 10 μM (Figure 3A).

On the basis of the correlation analysis (Figure 3D), hESC cardiomyocyte induction apparently strongly paralleled Wnt inhibition, and that is apparent in SAR studies. Even minor variations in the norbornene part of the molecule (region C) led to a loss of functional activity for both Wnt inhibition and hESC cardiogenesis. For example, the two-carbon-bridge analogue **37** and oxa bridge analogue **39** had IC_{50} values of 314 and 605 nM, respectively, in the Wnt inhibition assay and stimulated cardiogenesis only to the extent of less than 5%. The more potent compounds **9** (one-carbon-bridge analogue) and

10 (saturated version) had IC_{50} values of 24 and 4 nM, respectively, in the Wnt assay and induced cardiogenesis of 75% and 145%, respectively, compared to **1**. The effect of stereochemistry of the central portion of the molecule (region B) on the stereoselectivity of the biological end points was examined. The cis- and trans-configurations of the saturated cyclohexyl linker (region B) had similar effects on cardiogenesis and Wnt inhibition. For example, **28** (trans) and **56** (cis) had cardiogenesis of 78% and 72%, respectively (Figure 3B), and were relatively potent at Wnt inhibition (IC_{50} values of 6 and 23 nM respectively, Table 3). A number of alternate positions of the nitrogen in the quinoline heterocycle were tolerated for functional biological activity, but complete omission of the nitrogen atom led to a dramatic decrease in induction of cardiogenic potency (**12**, 41% Wnt inhibition at 1 μM and 8% cardiogenesis). Finally, different phenyl- and pyridinyl-substituted analogues gave comparable functional activity for induction of cardiogenesis and this showed that the quinoline could be replaced while retaining cardiogenesis induction. In particular, ortho substitution of phenyl and pyridinyl residues with carbonyl-containing groups afforded highly potent derivatives, and those analogues (**28**, **29**, and **34**) were among the most potent and effective compounds tested.

Finally, we tested potent Wnt inhibitors for selective inhibition of transforming growth factor β (TGFβ) signaling to investigate possible off-target effects. TGFβ interacts with Wnt to modulate stem cell fate,[18] and inhibition of TGFβ signaling can also be cardiogenic in mouse[19] and human ESCs.[20] Therefore, 10 representative structurally distinct compounds (**1**, **10**, **28**, **32**, **34**, **35**, **29**, **53**, **34**, and **35**) were incubated at concentrations varying from 0.01 to 5 μM (same dose range used in the Wnt assay) in a Smad response element−reporter assay in HEK293T cells stimulated with human recombinant TGFβ2. No significant inhibition effect was observed compared to DMSO vehicle controls even at the highest concentrations examined (inhibition of Smad response <20% at 0.01, 0.1, 1, and 5 μM; see Figure S3 in Supporting Information), indicating that TGFβ inhibition is not involved in the cardiac phenotype of the IWR-1 analogues examined. Furthermore, because the functional biological activity of **1** has been attributed to Axin stabilization, these data also indicate that Axin stabilization does not inhibit TGFβ/Smad signaling.

■ CONCLUSION

Enhancing the production of human cardiomyocytes offers a wealth of opportunities for drug research and toxicological assessment of new chemical entities. The Wnt pathway has been associated with cardiogenesis, and using **1** as a "lead", we obtained small-molecule Wnt inhibitors with IC_{50} values ranging from low nanomolar (4 nM) to the micromolar range. We showed a direct (i.e., titratable) correlation between Wnt inhibitory potency as determined by IC_{50} values in mammalian cells and cardiogenic functional activity in a human ESC-based assay. We were also able to improve the percentage of cardiogenesis to 176% with compound **29** compared to 100% for the initial "lead" **1** at much lower concentrations (i.e., 150 nM for **29** compared to 5000 nM for **1**, equivalent to 30-fold greater potency), rendering **29** more amenable to in vitro and in vivo applications. Because adult hearts contain cardiogenic progenitor cells that resemble the hESC-derived progenitor cells used in assays described herein in terms of gene expression profile and developmental potential,[4] it is possible that Wnt inhibition could promote differentiation of adult human cardiac progenitor cells. Therefore, an important next step will be to explore their utility for ex vivo expansion of adult heart-derived progenitors and to nominate and evaluate optimal compounds for their potential as in vivo regenerative compounds in animal models of myocardial infarction.

■ EXPERIMENTAL SECTION

General. Reagents and solvents were used as received from commercial sources. Compound **2** was purchased from Cayman Chemicals, **4** from Princeton BioMolecular Research, and **5** from Sigma−Aldrich. Synthetic products were isolated on a flash column chromatography system (Teledyne ISCO, CombiFlash Rf) with UV detection at 254 nm or PTLC (preparative thin-layer chromatography) with UV indicator. NMR (nuclear magnetic resonance) spectra were recorded at 300 MHz (^{1}H) on a Varian Mercury 300 or at 125 MHz (^{13}C) on a Bruker AMX-500 II (NuMega Resonance Lab, San Diego, CA). Chemical shifts were reported as parts per million, ppm (δ), relative to the solvent ($CDCl_3$ at 7.26 ppm, CD_3OD at 3.31 ppm, DMSO-d_6 at 2.50 and 3.52 ppm): s stands for singlet, d for doublet, t for triplet, q for quadruplet, m for multiplet, and br for broad. Low-resolution mass spectra were obtained on a Hitachi M-8000 mass spectrometer with an electrospray ionization (ESI) source.

Purity of final products was determined with a Hitachi 8000 LC-MS (Hitachi) using reverse-phase chromatography (C18 column, 50 × 4.6 mm, 5 μm, Thomson Instrument Co., Oceanside, CA). Compounds were eluted with gradient elution of 95/5 to 5/95 A/B over 5 min at a flow rate of 1.5 mL/min, where solvent A was water with 0.05% trifluoroacetic acid (TFA), and solvent B was acetonitrile with 0.05% TFA. For purity analysis, peak area percent for the TIC (total ion count) at 254 nm and retention time (t_R in minutes) were provided. Purity of final products was ≥95%.

Biological Assays. *Wnt Inhibition.* Compounds were tested for their ability to inhibit the β-catenin-dependent canonical Wnt pathway. A Wnt assay was adapted from Chen et al.[7] in our laboratories, with HEK293T cells in a 96-well format. Briefly, the commercially available Super(8×)TOPflash vector driven by a (7×)TCF-firefly luciferase response element was transiently transfected into HEK293T cells together with a TK-driven Renilla luciferase plasmid as an internal control to normalize the luminescence signal and a Wnt3A-expressing vector as the source of pathway activation. Because of the transient nature of the assay and, consequently, variations between independent experiments, **1** was included as a positive control in parallel with untreated and DMSO-treated vehicle controls in experiments conducted. Maximum inhibition of Wnt response in the assay format was around 90%, with the most potent inhibitors at the highest doses examined. Nonlinear regression analysis was performed with the log(inhibitor)/normalized response equation of the Prism 5 software.

hESC Cardiogenesis. Human embryonic stem cell H9 lines carrying MYH6-mCherry reporters were used in the hESC assay, as previously described in detail[6] and summarized in the Supporting Information. In brief, embryoid bodies (EB) were grown until day 4, dissociated gently to single cells, and transferred to 384-well plates. Concomitantly, different dilutions of small molecules were added. At day 10, medium was exchanged for a serum-free medium (SFM) containing the thyroid hormone analogue triiodothyronine T3 to increase the red signal driven by the MYH6 promoter for improved image analysis.[21] Cells were changed to phosphate-buffered saline (PBS) at day 14 for imaging, and red fluorescence images were collected on a high-throughput microscope. For quantifying the level of cardiac induction, the total area and intensity of the MYH6-mCherry reporter was measured in each well. Cardiac activity was reported by stating either percent cardiogenesis normalized to **1** (set as 100% at its maximum potency) or *Z* scores (relative to DMSO control) (Figure 3A and B).

Chemistry. Compounds **1** and **3** were synthesized following the procedure described in ref 7 and their ^{1}H NMR compared to the literature spectra.[7]

General Procedure for Intermediates ***8***. Triethylamine (0.92 mL, 6.6 mmol) and the desired anhydride **7** (6 mmol) were added to a solution of 4-amino acid **6** (6 mmol) in 5 mL of *N,N*-

dimethylformamide (DMF). The solution was heated for 16 h at 120 °C. After it returned to room temperature, the solvent was evaporated. The residue was then dissolved in ethyl acetate (100 mL) and washed with 1 N HCl (20 mL). The organic layer was washed with brine (25 mL) and dried with anhydrous magnesium sulfate. The solution was filtered to yield the desired intermediate **8** that was then used directly or purified by liquid chromatography.

*4-endo-Dihydronorbornylbenzoic Acid (**8a**).* Beige solid, 84% yield; (DCM)/MeOH 9/1 R_f 0.5; ^{1}H NMR (300 MHz, CD_3OD) 1.41 (d, J = 8.4 Hz, 2H), 1.61−1.69 (m, 4H), 2.89 (br s, 2H), 3.26 (br s, 2H), 7.41 (d, J = 8.7 Hz, 2H), 8.04 (s, OH), 8.19 (d, J = 8.7 Hz, 2H).

*4-(endo-Dihydronorbornyl)-trans-cyclohexanecarboxylic Acid (**8b**).* White solid, 35% yield; DCM/MeOH 9/1 R_f 0.8; LC-MS [1000 (+)-5.5−254−95:5] t_R 3.49 min, 246.02 [M − COOH], 291.75 [M + H]; ^{1}H NMR (300 MHz, $CDCl_3$) 1.25 (d, J = 8.4 Hz, 2H), 1.46−1.69 (m, 8H), 2.13 (d, J = 11.7 Hz, 2H), 2.21−2.44 (m, 3H), 2.74 (br s, 2H), 2.99 (br s, 2H), 3.98 (tt, J = 12.1 and 3 Hz, 1H), 8.01 (s, OH).

*4-(endo-Dihydronorbornyl)-cis-cyclohexanecarboxylic Acid (**8c**).* White solid, 73% yield; hexanes/EtOAc 1/1, R_f 0.4; LC-MS [1000 (+)-5.5−254−95:5] t_R 3.49 min, 246.02 [M − COOH], 291.75 [M + H]; ^{1}H NMR (300 MHz, $CDCl_3$) 1.23 (d, J = 8.4 Hz, 2H), 1.46−1.62 (m, 8H), 2.28−2.45 (m, 5H), 2.71 (br s, 2H), 2.97 (br s, 2H), 3.96 (tt, J = 12.1 and 3 Hz, 1H), 8.01 (s, 1H).

*4-cis-endo-(3a,4,7,7a-Tetrahydro-1H-4,7-ethanoisoindole-1,3(2H)-dion-2-yl)-benzoic Acid (**8d**).* Off-white solid, 99% yield; DCM/MeOH 9/1 R_f 0.2; ^{1}H NMR (300 MHz, DMSO) 1.61−1.38 (m, 4H), 2.16 (s, 2H), 2.92 (s, 2H), 7.41 (d, J = 8.4 Hz, 2H), 8.05 (d, J = 8.7 Hz, 2H), 13.15 (br s, 1H).

*4-cis−endo-[Hexahydro-1H-4,7-ethanoisoindole-1,3(2H)-dion-2-yl]benzoic Acid (**8e**).* White solid, 12% yield; DCM/MeOH 9/1 R_f 0.3; ^{1}H NMR (300 MHz, $CDCl_3$) 1.68−1.61 (m, 4H), 2.16 (s, 2H), 2.92 (s, 2H), 3.25−3.23 (m, 4H), 8.06−8.03 (m, 2H), 7.29−7.26 (m, 2H).

*General Procedure for Compounds **9**−**39** and **53**−**56**.* Synthesis of compounds **9**−**39** and **53**−**56** is illustrated in Scheme 1. Compounds were prepared in a library fashion. One gram of the appropriate intermediate **8** was heated for 16 h in 5 mL of thionyl chloride at 70 °C. TLC (DCM/MeOH 9/1) of a reaction aliquot diluted in methanol showed complete conversion to the methyl ester. Excess thionyl chloride was removed to afford the acid chloride. The acid chloride was dissolved in 20 mL of dichloroethane (DCE). A portion (0.3 mL) of the DCE solution was added to 30 mg of the appropriate amine and 0.1 mL of pyridine. Solutions were heated at 50 °C for 16 h, and the crude material was purified by liquid chromatography.

*4-(cis−endo-1,3-Dioxooctahydro-2H-4,7-methanoisoindol-2-yl)-N-(quinolin-8-yl)benzamide (**9**).* White solid, 51% yield; hexanes/EtOAc 3/7 R_f 0.6; LC-MS [1000 (+)-5.5−254−95:5] t_R 2.79 min, 411.95 [M + H] 96.3% at 254 nm; ^{1}H NMR (300 MHz, $CDCl_3$) 1.49 (d, J = 8.4 Hz, 2H), 1.58−1.79 (m, 4H), 2.90 (br s, 2H), 3.29 (br s, 2H), 7.47−7.63 (m, 5H), 8.16−8.23 (m, 3H), 8.84 (dd, J = 4.2 and 1.5 Hz, 1H), 8.92 (dd, J = 6.9 and 1.8 Hz, 1H), 10.79 (br s, NH).

*4-(cis−endo-1,3-Dioxooctahydro-2H-4,7-methanoisoindol-2-yl)-N-(quinolin-8-yl)-trans-cyclohexylcarboxamide (**10**).* Off-white solid, 55% yield; hexanes/EtOAc 1/1, R_f 0.4; LC-MS [1000 (+)-5.5−254−95:5] t_R 5.43 min, 418.02 [M + H] 96.3% at 254 nm; ^{1}H NMR (300 MHz, $CDCl_3$) 1.28 (d, J = 8.4 Hz, 2H), 1.53−1.64 (m, 4H), 1.71−1.85 (m, 4H), 2.21 (br d, J = 12.3 Hz, 2H), 2.42 (br q, J = 12.6 and 3.6 Hz, 2H), 2.56 (tt, J = 12 and 3.3 Hz, 1H), 2.76 (br s, 2H), 3.01 (br s, 2H), 4.09 (tt, J = 12.3 and 3.9 Hz, 1H), 7.43−7.55 (m, 3H), 8.15 (dd, J = 8.1 and 1.5 Hz, 1H), 8.76 (dd, J = 6.9 and 2.1 Hz, 1H), 8.81 (dd, J = 3.9 and 1.5 Hz, 1H), 9.92 (br s, 1H).

*4-(cis−endo-1,3-Dioxooctahydro-2H-4,7-methanoisoindol-2-yl)-N-(quinolin-8-yl)-cis-cyclohexylcarboxamide (**11**).* Transparent oil, 50% yield; hexanes/EtOAc 1/1, R_f 0.4; LC-MS [1000 (+)-5.5−254−95:5] t_R 3.35 min, 418.02 [M + H] 97.4% at 254 nm; ^{1}H NMR (300 MHz, $CDCl_3$) 1.26 (d, J = 8.4 Hz, 2H), 1.46−1.59 (m, 4H), 1.71−1.85 (m, 4H), 2.18 (br d, J = 12.3 Hz, 2H), 2.34−2.75 (m, 5H), 2.94 (br s, 1H), 3.00 (br s, 1H), 3.98−4.09 (m, 1H), 7.43−7.55 (m, 3H), 8.13 (dd, J = 8.1 and 1.5 Hz, 1H), 8.72−8.82 (m, 2H), 9.89 + 10.07 (br s, 1H).

*4-(cis−endo-1,3-Dioxooctahydro-2H-4,7-methanoisoindol-2-yl)-N-(naphthalen-1-yl)benzamide (**12**).* Off-white solid, 56% yield; hexanes/EtOAc 1/1, R_f 0.6; LC-MS [1000 (+)-5.5−254−95:5] t_R 3.81 min, 410.88 [M + H] 95.3% at 254 nm; ^{1}H NMR (300 MHz, $CDCl_3$) 1.41−1.51 (m, 2H), 1.58−1.79 (m, 4H), 2.89 (br s, 2H), 3.28 (br s, 2H), 7.46−7.61 (m, 5H), 7.77 (d, J = 8.7 Hz, 1H), 7.86−7.95 (m, 2H), 8−8.12 (m, 3H), 8.24 (br s, 1H).

*4-(cis−endo-1,3-Dioxooctahydro-2H-4,7-methanoisoindol-2-yl)-N-(isoquinolin-1-yl)-trans-cyclohexylcarboxamide (**13**).* White solid, 51% yield; DCM/MeOH 9/1 R_f 0.7; LC-MS [1000 (+)-5.5−254−95:5] t_R 4.84 min, 418.02 [M + H] 99.6% at 254 nm; ^{1}H NMR (300 MHz, $CDCl_3$ + CD_3OD) 1.22 (d, J = 8.4 Hz, 2H), 1.51−1.61 (m, 4H), 1.65−1.77 (m, 4H), 2.16 (d, J = 11.7 Hz, 2H), 2.21−2.44 (m 3H), 2.70 (br s, 2H), 2.98 (br s, 2H), 4.03 (tt, J = 12.1 and 3 Hz, 1H), 7.43 (br d, J = 5.4 Hz, 2H), 7.53−7.59 (m, 1H), 7.67 (dt, J = 6.9 and 0.9 Hz, 1H), 7.76 (d, J = 8.1 Hz, 1H), 8.06 (br s, 1H).

*4-(cis−endo-1,3-Dioxooctahydro-2H-4,7-methanoisoindol-2-yl)-N-(isoquinolin-4-yl)-trans-cyclohexylcarboxamide (**14**).* Yellow solid, 16% yield; DCM/MeOH 9/1 R_f 0.4; LC-MS [1000 (+)-5.5−254−95:5] t_R 4.10 min, 418.02 [M + H] 99.9% at 254 nm; ^{1}H NMR (300 MHz, $CDCl_3$+CD_3OD) 1.25 (d, J = 8.4 Hz, 2H), 1.51−1.61 (m, 4H), 1.65−1.77 (m, 4H), 2.15 (br d, J = 12.3 Hz, 2H), 2.25−2.43 (m, 3H), 2.74 (br s, 2H), 2.99 (br s, 2H), 3.99 (tt, J = 12.3 and 3.9 Hz, 1H), 7.58−7.73 (m, 3H), 7.82 (d, J = 8.4 Hz, 1H), 7.94 (d, J = 8.1 Hz, 1H), 8.04 (br s, 1H), 8.74 (s, NH).

*4-(cis−endo-1,3-Dioxooctahydro-2H-4,7-methanoisoindol-2-yl)-N-(quinolin-4-yl)-trans-cyclohexylcarboxamide (**15**).* Off-white solid, 5% yield; LC-MS [1000 (+)-5.5−254−95:5] t_R 2.75 min, 417.88 [M + H] 99.4% at 254 nm.

*4-(cis−endo-1,3-Dioxooctahydro-2H-4,7-methanoisoindol-2-yl)-N-(quinolin-5-yl)-trans-cyclohexylcarboxamide (**16**).* White solid, 40% yield; DCM/MeOH 9/1, R_f 0.4; LC-MS [1000 (+)-5.5−254−95:5] t_R 4.20 min, 418.02 [M + H] 99.5% at 254 nm; ^{1}H NMR (300 MHz, $CDCl_3$) 1.25 (d, J = 8.4 Hz, 2H), 1.53−1.64 (m, 4H), 1.71−1.85 (m, 4H), 2.17 (br d, J = 12.3 Hz, 2H), 2.21−2.49 (m, 3H), 2.72 (br s, 2H), 2.99 (br s, 2H), 4.08 (tt, J = 12.3 and 3.9 Hz, 1H), 7.42 (dd, J = 8.4 and 3.9 Hz, 1H), 7.66−7.83 (m, 2H), 7.98 (d, J = 7.5 Hz, 1H), 8.17 (d, J = 8.4 Hz, 1H), 8.92 (d, J = 4.5 Hz, 1H), 8.82 (br s, 1H).

*4-(cis−endo-1,3-Dioxooctahydro-2H-4,7-methanoisoindol-2-yl)-N-(isoquinolin-5-yl)-trans-cyclohexylcarboxamide (**17**).* Yellow glassy solid, 72% yield; DCM/MeOH 9/1, R_f 0.7; LC-MS [1000 (+)-5.5−254−95:5] t_R 3.27 min, 418.02 [M + H] 92.9% at 254 nm; ^{1}H NMR (300 MHz, $CDCl_3$) 1.28 (d, J = 8.4 Hz, 2H), 1.53−1.64 (m, 4H), 1.71−1.85 (m, 4H), 2.22 (br d, J = 12.3 Hz, 2H), 2.24−2.58 (m, 3H), 2.71 (br s, 2H), 2.99 (br s, 2H), 4.08 (tt, J = 12.3 and 3.9 Hz, 1H), 7.55−7.64 (m, 2H), 7.79 (d, J = 8.4 Hz, 1H), 7.95 (s, 1H), 8.13 (d, J = 7.8 Hz, 1H), 8.53 (d, J = 6.3 Hz, 1H), 9.24 (s, 1H).

*4-(cis−endo-1,3-Dioxooctahydro-2H-4,7-methanoisoindol-2-yl)-N-(isoquinolin-8-yl)-trans-cyclohexylcarboxamide (**18**).* Yellow solid, 16% yield; DCM/MeOH 9/1, R_f 0.8; LC-MS [1000 (+)-5.5−254−95:5] t_R 4.04 min, 418.02 [M + H] 90.1% at 254 nm; ^{1}H NMR (300 MHz, $CDCl_3$) 1.27 (d, J = 6.9 Hz, 2H), 1.53−1.69 (m, 4H), 1.71−1.88 (m, 4H), 2.20 (br d, J = 12.4 Hz, 2H), 2.24−2.58 (m, 4H), 2.73 (br s, 2H), 3.00 (br s, 2H), 4.01−4.16 (m, 1H), 7.57−7.64 (m, 2H), 8.00−8.06 (m, 1H), 8.20 (br s, 1H), 8.53 (d, J = 5.8 Hz, 1H), 9.43 (s, NH).

*4-(cis−endo-1,3-Dioxooctahydro-2H-4,7-methanoisoindol-2-yl)-N-(p-tolyl)benzamide (**19**).* Off-white solid, 14% yield; hexanes/EtOAc 1/1, R_f 0.6; LC-MS [1000 (+)-5.5−254−95:5] t_R 4.55 min, 374.88 [M + H] 98.5% at 254 nm; ^{1}H NMR ($CDCl_3$) 1.46 (d, J = 8.4 Hz, 2H), 1.53−1.74 (m, 4H), 2.34 (s, 3H), 2.89 (br s, 2H), 3.27 (br s, 2H), 7.18 (d, J = 8.1 Hz, 2H), 7.41 (d, J = 8.7 Hz, 2H), 7.51 (d, J = 8.1 Hz, 2H), 7.79 (br s, 1H), 7.95 (d, J = 8.4 Hz, 2H).

*4-(cis−endo-1,3-Dioxooctahydro-2H-4,7-methanoisoindol-2-yl)-N-(4-methoxyphenyl) benzamide (**20**).* Gray solid, 20% yield; hexanes/EtOAc 1/1, R_f 0.4; LC-MS [1000 (+)-5.5−254−95:5] t_R 3.73 min, 390.82 [M + H] 93.4% at 254 nm; ^{1}H NMR ($CDCl_3$) 1.19−1.26 (m, 2H), 1.45−1.74 (m, 4H), 2.89 (br s, 2H), 3.27 (br s, 2H), 3.82 (s, 3H), 6.91 (d, J = 8.4 Hz, 2H), 7.41 (d, J = 8.4 Hz, 2H), 7.54 (d, J = 8.4 Hz, 2H), 7.78 (s, NH), 7.95 (d, J = 8.4 Hz, 2H).

*2-cis–endo-(1,3-Dioxooctahydro-2H-4,7-methanoisoindol-2-yl)-N-(2-methoxyphenyl)benzamide (**21**).* White solid, 91% yield; hexanes/EtOAc 3/7, R_f 0.6; LC-MS [1000 (+)-5.5–254–95:5] t_R 4.12 min, 390.35 [M + H] 100% at 254 nm; ^{1}H NMR (300 MHz, $CDCl_3$) 1.47 (d, J = 8.4 Hz, 2H), 1.58–1.79 (m, 4H), 2.89 (br s, 2H), 3.28 (br s, 2H), 3.92 (s, 3H), 6.92 (dd, J = 7.8 and 1.2 Hz, 1H), 6.99–7.13 (m, 2H), 7.41–7.45 (m, 2H), 7.97–8.02 (m, 2H), 8.51 (dd, J = 7.8 and 1.2 Hz, 1H), 8.52 (br s, 1H).

*2-cis–endo-(1,3-Dioxooctahydro-2H-4,7-methanoisoindol-2-yl)-N-(4-(dimethylamino)phenyl)benzamide (**22**).* Dark green solid, 36% yield; DCM/MeOH 9/1, R_f 0.2; LC-MS [1000 (+)-5.5–254–95:5] t_R 2.17 min, 403.95 [M + H] 99.6% at 254 nm; ^{1}H NMR ($CDCl_3$) 1.46 (d, J = 8.4 Hz, 2H), 1.59–1.76 (m, 4H), 2.88 (br s, 2H), 2.94 (s, 6H), 3.27 (br s, 2H), 6.74 (d, J = 9.3 Hz, 2H), 7.38 (d, J = 8.1 Hz, 2H), 7.48 (d, J = 9.3 Hz, 2H), 7.74 (s, NH), 7.94 (d, J = 8.1 Hz, 2H).

*2-cis–endo-(1,3-Dioxooctahydro-2H-4,7-methanoisoindol-2-yl)-N-(4-cyanophenyl)benzamide (**23**).* White solid, 48% yield; DCM/MeOH 95/5, R_f 0.1; LC-MS [1000 (+)-5.5–254–95:5] t_R 3.48 min, 347.68 [M + H] 90%; ^{1}H NMR ($CDCl_3$ + CD_3OD) 1.33 (d, J = 8.4 Hz, 2H), 1.55–1.69 (m, 5H), 2.77 (br s, 2H), 3.20 (br s, 1H), 7.26 (d, J = 8.2 Hz, 2H), 7.53 (d, J = 9.1 Hz, 2H), 7.77 (d, J = 9.1 Hz, 2H), 7.90 (d, J = 8.8 Hz, 2H).

*2-cis–endo-(1,3-Dioxooctahydro-2H-4,7-methanoisoindol-2-yl)-N-(4-acetylphenyl)benzamide (**24**).* Off-white solid, 35% yield; DCM/MeOH 95/5, R_f 0.4; LC-MS [1000 (+)-5.5–254–95:5] t_R 2.98 min, 402.84 [M + H] 97.9% at 254 nm.

*4-(cis–endo-1,3-dioxooctahydro-2H-4,7-methanoisoindol-2-yl)-N-(2-hydroxyphenyl)-trans-cyclohexylcarboxamide (**25**).* Orange solid, 43% yield; hexanes/EtOAc 1/1, R_f 0.4; LC-MS [1000 (+)-5.5–254–95:5] t_R 3.01 min, 418 [M + H] 99% at 254 nm; ^{1}H NMR (300 MHz, CD_3OD) 1.23 (d, J = 8.4 Hz, 2H), 1.53–1.71 (m, 4H), 1.75–2.01 (m, 4H), 2.06 (br d, J = 12.3 Hz, 2H), 2.28–2.35 (m, 3H), 2.72 (br s, 2H), 2.98 (br s, 2H), 3.98–4.14 (m, 1H), 6.76–6.87 (m, 2H), 6.96 (dd, J = 7.98 and 1.5 Hz, 1H), 7.58 (dd, J = 7.98 and 1.5 Hz, 1H).

*4-(cis_-endo-1,3-Dioxooctahydro-2H-4,7-methanoisoindol-2-yl)-N-(2-ethoxyphenyl)-trans-cyclohexylcarboxamide (**26**).* White solid, 73% yield; hexanes/EtOAc 1/1, R_f 0.6; LC-MS [1000 (+)-5.5–254–95:5] t_R 3.46 min, 418 [M + H] 99% at 254 nm; ^{1}H NMR (300 MHz, $CDCl_3$) 1.23 (d, J = 8.4 Hz, 2H), 1.53–1.71 (m, 10H), 2.06 (br d, J = 12.3 Hz, 2H), 2.28–2.35 (m, 4H), 2.72 (br s, 2H), 2.98 (br s, 2H), 3.98–4.14 (m, 3H), 6.83 (dd, J = 7.5 and 1.5 Hz, 1H), 6.87–7.11 (m, 2H), 7.85 (br s, NH), 8.34 (dd, J = 7.5 and 1.5 Hz, 1H).

*Methyl 2-[4-(cis–endo-1,3-dioxooctahydro-2H-4,7-methanoisoindol-2-yl)]-N-trans-cyclohexanecarboxamido)benzoate (**27**).* White solid, 58% yield; DCM/MeOH 95/5 R_f 0.8; LC-MS [1000 (+)-5.5–254–95:5] t_R 3.58 min, 418 [M + H] 92.4% at 254 nm; ^{1}H NMR (300 MHz, $CDCl_3$) 1.24 (d, J = 8.4 Hz, 2H), 1.51–1.72 (m, 8H), 2.14 (br d, J = 11.7 Hz, 2H), 2.26–2.41 (m, 3H), 2.73 (br s, 2H), 2.99 (br s, 2H), 3.91 (s, 3H), 4.03 (t, J = 12.6 Hz, 1H), 7.05 (t, J = 7.8 Hz, 1H), 7.51 (t, J = 8.7 Hz, 1H), 8 (dd, J = 7.8 and 1.2 Hz, 1H), 8.71 (d, J = 8.7 Hz, 1H), 11.15 (br s, 1H).

*4-(cis–endo-1,3-Dioxooctahydro-2H-4,7-methanoisoindol-2-yl)-N-(2-acetylphenyl)-trans-cyclohexylcarboxamide (**28**).* Brown solid, 38% yield; hexanes/EtOAc 1/1, R_f: 0.4; LC-MS [1000 (+)-5.5–254–95:5] t_R 4.40 min, 408.28 [M + H] 94.7% at 254 nm; ^{1}H NMR (300 MHz, $CDCl_3$) 1.26 (d, J = 8.4 Hz, 2H), 1.53–1.85 (m, 8H), 2.16 (br d, J = 12.3 Hz, 2H), 2.28–2.49 (m, 3H), 2.67 (s, 3H), 2.75 (br s, 2H), 3.01 (br s, 2H), 4.08 (tt, J = 12.3 and 3.9 Hz, 1H), 7.11 (t, J = 7.5 Hz, 1H), 7.55 (t, J = 8.7 and 1.5 Hz, 1H), 7.90 (dd, J = 7.8 and 1.2 Hz, 1H), 8.76 (d, J = 8.4 Hz, 1H), 11.84 (s, NH).

*4-[cis–endo-(1,3-Dioxooctahydro-2H-4,7-methanoisoindol-2-yl)]-N-(8-oxo-5,6,7,8-tetrahydronaphthalen-1-yl)-trans-cyclohexylcarboxamide (**29**).* Brown oil, 51% yield; hexanes/EtOAc 1/1, R_f 0.6; LC-MS [1000 (+)-5.5–254–95:5] t_R 3.73 min, 434.48 [M + H] 97.5% at 254 nm; ^{1}H NMR (300 MHz, $CDCl_3$) 1.21 (d, J = 8.4 Hz, 2H), 1.53–1.67 (m, 8H), 2.07–2.15 (m, 4H), 2.19–2.54 (m, 3H), 2.61–2.78 (m, 4H), 2.88–3.-02 (m, 4H), 3.98–4.14 (m, 1H), 6.91 (dd, J = 7.5 and 1.5 Hz, 1H), 7.42 (t, J = 7.5 Hz, 1H), 8.60 (dd, J = 7.5 and 1.5 Hz, 1H), 12.23 (br s, 1H).

*4-[cis–endo-(1,3-Dioxooctahydro-2H-4,7-methanoisoindol-2-yl)]-N-(9H-fluoren-9-on-1-yl)-trans-cyclohexylcarboxamide (**30**).* Yellow solid, 46% yield; DCM/MeOH 95/5, R_f 0.7; LC-MS [1000 (+)-5.5–254–95:5] t_R 4.38 min, 469 [M + H] 99.4% at 254 nm; ^{1}H NMR (300 MHz, $CDCl_3$) 1.26 (d, J = 8.4 Hz, 2H), 1.47–1.74 (m, 8H), 2.18 (br d, J = 11.7 Hz, 2H), 2.26–2.48 (m, 3H), 2.75 (br s, 2H), 3.00 (br s, 2H), 4.04 (t, J = 12.6 Hz, 1H), 7.15 (t, J = 7.2 Hz, 1H), 7.25–7.31 (m, 1H), 7.38–7.47 (m, 3H), 7.58 (d, J = 7.5 Hz, 1H), 8.34 (d, J = 8.1 Hz, 1H), 10.17 (br s, NH).

*4-[cis–endo-(1,3-Dioxooctahydro-2H-4,7-methanoisoindol-2-yl)]-N-(pyridin-2-yl)-trans-cyclohexylcarboxamide (**31**).* Off-white solid, 6% yield; DCM/MeOH 9/1, R_f 0.7; LC-MS [1000 (+)-5.5–254–95:5] t_R 1.27 min, 367.88 [M + H] 97.5% at 254 nm; ^{1}H NMR (300 MHz, $CDCl_3$) 1.26 (d, J = 8.4 Hz, 2H), 1.51–1.74 (m, 9H), 2.09 (br d, J = 11.7 Hz, 2H), 2.26–2.39 (m, 2H), 2.75 (br s, 2H), 3.01 (br s, 2H), 4.01–4.17 (m, 1H), 7.01–7.05 (m, 1H), 7.69 (dt, J = 9 and 2.1 Hz, 1H), 7.99 (br s, NH), 8.21 (d, J = 8.7 Hz, 1H), 8.24–8.27 (m, 1H).

*4-[cis–endo-(1,3-Dioxooctahydro-2H-4,7-methanoisoindol-2-yl)]-N-(pyridin-3-yl)-trans-cyclohexylcarboxamide (**32**).* White solid, 32% yield; DCM/MeOH 9/1, R_f 0.8; LC-MS [1000 (+)-5.5–254–95:5] t_R 2.46 min, 367.88 [M + H] 97.9% at 254 nm; ^{1}H NMR (300 MHz, $CDCl_3$ + 1 drop of CD_3OD) 1.28 (d, J = 8.4 Hz, 2H), 1.53–1.64 (m, 4H), 1.71–1.85 (m, 4H), 1.86 (br d, J = 12.3 Hz, 2H), 2.12–2.38 (m, 3H), 2.76 (br s, 2H), 3.01 (br s, 2H), 4.08 (tt, J = 12.3 and 3.9 Hz, 1H), 7.21 (dd, J = 8.4 and 3.6 Hz, 1H), 8.14 (br d, J = 3.6 Hz, 1H), 8.20 (br d, J = 8.4 Hz, 1H), 8.42 (d, J = 2.1 Hz, 1H).

*4-[cis–endo-(1,3-Dioxooctahydro-2H-4,7-methanoisoindol-2-yl)]-N-(pyridin-4-yl)-trans-cyclohexylcarboxamide (**33**).* Yellow solid, 8% yield; DCM/MeOH 9/1, R_f 0.7; LC-MS [1000 (+)-5.5–254–95:5] t_R 1.68 min, 367.89 [M + H] 97.3% at 254 nm; ^{1}H NMR (300 MHz, $CDCl_3$) 1.25 (d, J = 8.4 Hz, 2H), 1.46–1.75 (m, 8H), 2.07 (br d, J = 12.3 Hz, 2H), 2.23–2.37 (m, 3H), 2.75 (br s, 2H), 3.02 (br s, 2H), 4.08 (tt, J = 12.3 and 3.9 Hz, 1H), 7.31 (br s, NH), 7.48 (d, J = 6.3 Hz, 2H), 8.50 (br d, J = 6.3 Hz, 2H).

*4-[cis–endo-(1,3-Dioxooctahydro-2H-4,7-methanoisoindol-2-yl)]-N-(2-acetylpyridin-3-yl)-trans-cyclohexylcarboxamide (**34**).* Off-white solid, 17% yield; hexanes/EtOAc 7/3, R_f 0.2; LC-MS [1000 (+)-5.5–254–95:5] t_R 4.35 min, 409.28 [M + H] 96.4% at 254 nm; ^{1}H NMR (300 MHz, $CDCl_3$) 1.26 (d, J = 8.8 Hz, 2H), 1.51–1.78 (m, 8H), 2.18 (br d, J = 11.8 Hz, 2H), 2.31–2.52 (m, 5H), 2.76 (br s, 1H), 2.80 (s, 3H), 3.03 (br s, 1H), 3.97–4.15 (m, 1H), 7.43–7.48 (m, 1H), 8.35 (dd, J = 4.4 and 0.9 Hz, 1H), 9.09 (dd, J = 8.8 and 0.9 Hz, 1H), 11.62 (br s, NH).

*4-[cis–endo-(1,3-Dioxooctahydro-2H-4,7-methanoisoindol-2-yl)]-N-(6-acetylpyridin-3-yl)-trans-cyclohexylcarboxamide (**35**).* Off-white solid, 18% yield; hexanes/EtOAc 7/3, R_f 0.2; LC-MS [1000 (+)-5.5–254–95:5] t_R 3.46 min, 409.48 [M + H] 98.6% at 254 nm; ^{1}H NMR (300 MHz, $CDCl_3$) 1.28 (d, J = 8.4 Hz, 2H), 1.49–1.78 (m, 8H), 2.17 (d, J = 11.7 Hz, 2H), 2.29–2.49 (m, 5H), 2.71 (s, 3H), 2.77 (br s, 1H), 2.99 (br s, 1H), 3.98–4.11 (m, 1H), 7.64 (d, J = 5.23 Hz, 1H), 8.47 (d, J = 5.53 Hz, 1H), 10.05 (s, 1H), 11.20 (s, NH).

*4-cis_-endo-[3a,4,7,7a-Tetrahydro-1H-4,7-ethanoisoindole-1,3(2H)-dion-2-yl]-N-quinolin-8-ylbenzamide (**36**).* Yellow solid, 10% yield; hexanes/EtOAc 1/1, R_f 0.3; LC-MS [1000 (+)-5.5–254–95:5] t_R 3.87 min, 423.68 [M + H] 96% at 254 nm; ^{1}H NMR (300 MHz, $CDCl_3$) 1.70–1.45 (m, 4H), 3.06 (s, 2H), 3.29 (br s, 2H), 6.33–6.31 (m, 2H), 7.60–7.41 (m, 5H), 8.21–8.14 (m, 3H), 8.85–8.83 (m, 1H), 8.93–8.90 (m, 1H), 10.74 (s, 1H).

*4-cis–endo-[Hexahydro-1H-4,7-ethanoisoindole-1,3(2H)-dion-2-yl]-N-quinolin-8-ylbenzamide (**37**).* White solid, 51% yield; hexanes/EtOAc 3/7, R_f 0.6; LC-MS [1000 (+)-5.5–254–95:5] t_R 2.79 min, 411.95 [M + H] 96.3% at 254 nm; ^{1}H NMR (300 MHz, DMSO) 1.48–1.53 (m, 4H), 1.66–1.68 (m, 4H), 2.08–2.10 (m, 2H), 3.08–3.10 (m, 2H), 7.55 (d, J = 8.8 Hz, 2H), 7.66–7.70 (m, 2H), 7.77 (dd, J = 8.4 and 1.5 Hz, 1H), 8.17 (d, J = 8.8 Hz, 2H), 8.48 dd, J = 8.4 and 1.5 Hz, 1H), 8.73 (dd, J = 8.4 and 1.5 Hz, 1H), 8.98–8.99 (m, 1H), 10.70 (br s, NH).

*4-(cis–endo-8-Methyl-1,3-dioxooctahydro-2H-4,7-methanoisoindol-2-yl)-N-quinolin-8-ylbenzamide (**38**).* Orange solid, 64% yield; hexanes/EtOAc 1/1, R_f 0.4; ^{1}H NMR (300 MHz, DMSO)

1.47 (d, J = 8.4 Hz, 1H), 1.58−1.79 (m, 1H), 1.83 (s, 3H), 3.28 (br s, 2H), 3.92 (s, 2H), 5.87 (s, 1H), 7.49−7.55 (m, 2H), 7.52−7.77 (m, 3H), 8.13 (d, J = 8.8 Hz, 2H), 8.45 (dd, J = 8.53 and 0.9 Hz, 1H), 8.69 (dd, J = 8.53 and 0.9 Hz, 1H), 8.95 (dd, J = 4.4 and 0.9 Hz, 1H).

*4-[Hexahydro-1H-4,7-epoxyisoindole-1,3(2H)-dion-2-yl]-N-quinolin-8-ylbenzamide (**39**).* 7-Oxabicyclo[2.2.1]heptane-2,3-dicarboxylic anhydride was prepared according to literature procedures.[22] Beige solid, 68% yield; DCM/MeOH 9/1, R_f 0.8; LC-MS [1000 (+)-5.5−254−95:5] t_R 3.23 min, 414 [M + H] >99% at 254 nm; ^{1}H NMR (300 MHz, $CDCl_3$) 1.68−1.75 (m, 2H), 1.94−1.98 (m, 2H), 3.11 (s, 2H), 5.05 (m, 2H), 7.47−7.63 (m, 5H), 8.16−8.19 (m, 2H), 8.21 (br d, J = 1.67 Hz, 1H), 8.85 (dd, J = 1.67, 4.21 Hz, 1H), 8.91 (dd, J = 1.89, 7.08 Hz, 1H), 10.75 (s, 1H).

*4-(cis−endo-1,3-Dioxooctahydro-2H-4,7-methanoisoindol-2-yl)-N-(4-bromo-2-methoxyphenyl)-trans-cyclohexylcarboxamide (**53**).* Off-white solid, 11% yield; DMC/MeOH 9/1, R_f 0.8; LC-MS [1000 (+)-5.5−254−95:5] t_R 3.98 min, 474.48−476.48 [M + H] 90.3% at 254 nm; ^{1}H NMR (300 MHz, $CDCl_3$) 1.11 (d, J = 8.4 Hz, 2H), 1.45−1.77 (m, 6H), 2.04 (br d, J = 12 Hz, 4H), 2.08−2.41 (m, 4H), 2.74 (br s, 2H), 2.99 (br s, 2H), 3.87 (s, 3H), 4.04 (t, J = 12.6 Hz, 1H), 7 (s, 1H), 7.07 (d, J = 7 Hz, 1H), 7.87 (br s, NH), 8.24 (d, J = 7 Hz, 1H).

*4-(cis−endo-1,3-Dioxooctahydro-2H-4,7-methanoisoindol-2-yl)-N-(5-hydroxylpyridin-3-yl)-trans-cyclohexylcarboxamide (**54**).* Beige solid, 21% yield; DCM/MeOH 9/1, R_f 0.7; LC-MS [1000 (+)-5.5−254−95:5] t_R 1.47 min, 383.88 [M + H] 97.2% at 254 nm; ^{1}H NMR (300 MHz, $CDCl_3$ + CD_3OD) 1.06 (d, J = 8.4 Hz, 2H), 1.39−1.59 (m, 6H), 1.82 (br d, J = 11.7 Hz, 2H), 2.06−2.38 (m, 3H), 2.58 (br s, 2H), 2.88 (br s, 2H), 4.04 (t, J = 12.6 Hz, 1H), 7.59 (s, 1H), 7.65 (s, 1H), 7.87 (s, 1H).

*4-(cis−endo-1,3-Dioxooctahydro-2H-4,7-methanoisoindol-2-yl)-N-(2-chloropyridin-3-yl)-trans-cyclohexylcarboxamide (**55**).* Pale yellow solid, 35% yield; DCM/MeOH 9/1, R_f 0.6; LC-MS [1000 (+)-5.5−254−95:5] t_R 2.91 min, 401.68 [M + H] 98.7% at 254 nm; ^{1}H NMR (300 MHz, $CDCl_3$) 1.26 (d, J = 8.4 Hz, 2H), 1.51−1.74 (m, 6H), 2.18 (br d, J = 11.7 Hz, 2H), 2.26−2.48 (m, 3H), 2.73 (br s, 2H), 3.00 (br s, 2H), 3.92−4.02 (m, 1H), 7.25 (dd, J = 8.4 and 4.9 Hz, 1H), 7.69 (br s, NH), 8.10 (dd, J = 4.9 and 1.8 Hz, 1H), 8.73 (dd, J = 8.4 and 1.8 Hz, 1H).

*4-(cis−endo-1,3-Dioxooctahydro-2H-4,7-methanoisoindol-2-yl)-N-(2-acetylphenyl)-cis-cyclohexylcarboxamide (**56**).* Beige wax, 40% yield; hexanes/EtOAc 1/1, R_f 0.5; LC-MS [1000 (+)-5.5−254−95:5] t_R 4.06 min, 408.42 [M + H] 96.2% at 254 nm; ^{1}H NMR (300 MHz, $CDCl_3$) 1.24 (d, J = 8.4 Hz, 2H), 1.48−1.79 (m, 7H), 2.29−2.46 (m, 5H), 2.64 (s, 3H), 2.72 (br s, 2H), 2.98 (br s, 2H), 3.97−4.08 (m, 1H), 7.07−7.13 (m, 1H), 7.54 (tt, J = 8.7 and 1.5 Hz, 1H), 7.89 (td, J = 8.1 and 1.5 Hz, 1H), 8.76 + 8.87 (dd, J = 8.7 and 0.9 Hz, 1H), 11.80 + 11.96 (br s, NH).

*3-(cis−endo-1,3-Dioxooctahydro-2H-4,7-methanoisoindol-2-yl)-N-quinolin-8-ylbenzamide (**45**).* Compound **45** was synthesized according to procedures described for compounds **9**−**39** and **53**−**56** but 4-aminobenzoic acid was replaced by 3-aminobenzoic acid. White solid, 96% yield; hexanes/EtOAc 1/1, R_f 0.4; LC-MS [1000 (+)-5.5−254−95:5] t_R 3.91 min, 411.82 [M + H] 98.9% at 254 nm; ^{1}H NMR (500 MHz, DMSO-d_6) 1.32−1.37 (m, 2H), 1.57−1.64 (m, 3H), 1.70−1.72 (m, 1H), 2.70−2.72 (m, 2H), 3.31−3.33 (m, 2H, overlaps with residual H_2O signal), 7.53−7.55 (m, 1H), 7.66−7.70 (m, 2H), 7.75−7.79 (m, 2H), 7.88−7.89 (m, 1H), 8.10−8.12 (m, 1H), 8.47 (dd, J = 8.4 and 1.5 Hz, 1H), 8.69 (dd, J = 8.4 and 1.5 Hz, 1H), 8.96−8.97 (m, 1H), 10.68 (br s, NH, 1H).

*5-(cis−endo-1,3-Dioxooctahydro-2H-4,7-methanoisoindol-2-yl)-N-quinolin-8-ylfuran-2-carboxamide (**46**).* Compound **46** was synthesized according to procedures described for compounds **41**−**44** but 4-nitrobenzoic acid was replaced by 5-nitrofuroic acid. Orange oil, 20% yield; DCM/MeOH 9/1, R_f 0.7; LC-MS [1000 (+)-5.5−254−95:5] t_R 4.12 min, 401.82 [M + H] 90% at 254 nm; ^{1}H NMR ($CDCl_3$) 1.2−1.82 (m, 5H), 2.92 (br s, 2H), 3.33 (br s, 2H), 7.36 (d, J = 3.6 Hz, 1H), 7.43−7.48 (m, 3H), 7.54−7.58 (m, 1H), 8.17 (dd, J = 8.25 and 1.65 Hz, 1H), 8.76 (dd, J = 6.9 and 2.1 Hz, 1H), 8.87 (dd, J = 3.9 and 1.5 Hz, 1H), 10.74 (br s, NH).

*N-(4-Nitrophenyl)-(3aR,4S,7R,7aS)-1,3,3a,4,7,7a-hexahydro-1,3-dioxo-4,7-methano-2H-isoindole (**51**).* Compound **51** (Scheme 5, step a) was synthesized according to the procedure described for intermediate **8** but starting from 1.64 g of carbic anhydride (10 mmol), 1.67 mL of triethylamine, and 1.52 g of 4-nitroaniline. Yellow solid, 52% yield; DCM/MeOH 9/1, R_f 0.6; LC-MS [1000 (+)-5.5−254−95:5] t_R 3.35 min, 96.8% at 254 nm; ^{1}H NMR (300 MHz, $CDCl_3$) 1.62−1.68 (m, 1H), 1.80−1.86 (m, 1H), 3.49 (dd, J = 1.63, 3.09 Hz, 2H), 3.55 (m, 2H), 6.27 (br t, J = 1.80 Hz, 2H), 7.40−7.44 (m, 2H), 8.26−8.31 (m, 2H).

N-(4-Aminophenyl)-(3aR,4S,7R,7aS)-1,3,3a,4,7,7a-hexahydro-1,3-dioxo-4,7-methano-2H-isoindole. As shown in Scheme 5, step b, 300 mg of **51** was dissolved in 30 mL of EtOH, and 40 mg of Pd/C (10%) was added. The mixture was stirred at room temperature for 16 h under a hydrogen atmosphere. The solution was filtered through a pad of Celite and concentrated to dryness. The crude product was purified by flash chromatography (hexanes/EtOAc 1/1, R_f 0.2) to afford 180 mg (67% yield). LC-MS [1000 (+)-10.0−254−95:5] t_R 3.14 min, 257 [M + H]; 98.8% at 254 nm. ^{1}H NMR (300 MHz, $CDCl_3$): 1.43−1.72 (m, 6H), 2.85 (m, 2H), 3.21 (m, 2H), 3.81 (br s, 2H, NH_2), 6.71−6.75 (m, 2H), 6.98−7.01 (m, 2H).

*N-{4-[(3aR,4S,7R,7aS)-1,3,3a,4,7,7a-Hexahydro-1,3-dioxo-4,7-methano-2H-isoindol-2-yl]phenyl}quinoline-8-carboxamide (**52**).* As shown in Scheme 5, step c, quinoline-8-carbonyl chloride was freshly prepared by treating 135 mg (0.78 mmol) of quinoline-8-carboxylic acid with an excess of thionyl chloride (622 μL) for 3 h at 60−70 °C. After the mixture returned to room temperature, excess thionyl chloride was removed by evaporation. The mixture was added dropwise to a solution of 100 mg of the aniline precursor from step b (0.39 mmol) and 5 equiv of triethylamine (1.95 mmol) in 7 mL of dry acetonitrile. The mixture was stirred at room temperature for 3 days, concentrated in a vacuum, and purified by flash chromatography (toluene/EtOAc/acetone 6/3/1, R_f 0.5). The product was obtained as an off-white solid in 87% yield (140 mg). LC-MS [1000 (+)-5.5−254−95:5] t_R 3.45 min, 412 [M + H] >99% at 254 nm; ^{1}H NMR (300 MHz, $CDCl_3$) 1.48−1.75 (m, 6H), 2.88 (m, 2H), 3.25 (m, 2H), 7.27−7.32 (m, 2H), 7.56 (dd, J = 4.3 and 8.3 Hz, 1H), 7.74 (dd, J = 7.45 and 7.50 Hz, 1H), 7.98−8.03 (m, 2H), 8.02 (br d, J = 1.6 Hz, 1H), 8.34 (dd, J = 1.8 and 8.4 Hz, 1H), 8.96 (dd, J = 1.6 and 7.4 Hz, 1H), 9.01 (dd, J = 1.8 and 4.3 Hz, 1H).

■ ASSOCIATED CONTENT

Supporting Information

Additional text, three figures, and one table showing analytical and spectral characterization data for all compounds obtained from Schemes 2−4, detailed hESC assay procedures, and data on cell viability/toxicity, TGFβ inhibition, and chemical stability for select compounds. This material is available free of charge via the Internet at http://pubs.acs.org.

■ AUTHOR INFORMATION

Corresponding Author

*E-mail mlanier@hbri.org; telephone 001 (858) 458-9305; fax 001 (858) 458-9311.

Author Contributions

[‖]These authors contributed equally.

■ ACKNOWLEDGMENTS

We thank Alyssa Morgosh and Claire Johns at HBRI for their technical assistance with compound preparation during their internship at HBRI, and Drs. Zebin Xia and Marcia I. Dawson (SBMRI) for kindly providing **3** for biological testing. We thank the NIH (R01HL059502 and R33HL088266 to M.M.) and the California Institute for Regenerative Medicine (CIRM, RC1-000132 to M.M.) and the T Foundation (to J.R.C.) for their generous financial support. We gratefully acknowledge postdoctoral fellowships from the German Research Founda-

tion (DFG) (to D.S.), and CIRM (TG-0004) and American Heart Association (to E.W.).

■ ABBREVIATIONS:

hERG, human ether-a-go-go-related gene; hESC, human embryonic stem cells; HCS, high content screen; HEK293T, human embryonic kidney 293T; IWR, inhibitor of Wnt response

■ REFERENCES

(1) Murata, M.; Tohyama, S.; Fukuda, K. Impacts of recent advances in cardiovascular regenerative medicine on clinical therapies and drug discovery. *Pharmacol. Ther.* **2010**, *126* (2), 109−118.

(2) Willems, E.; Lanier, M.; Forte, E.; Lo, F.; Cashman, J.; Mercola, M. A chemical biology approach to myocardial regeneration. *J. Cardiovasc. Transl. Res.* **2011**, *4* (3), 340−350.

(3) Sartipy, P.; Bjorquist, P.; Strehl, R.; Hyllner, J. The application of human embryonic stem cell technologies to drug discovery. *Drug Discovery Today* **2007**, *12* (17−18), 688−699.

(4) Mercola, M.; Ruiz-Lozano, P.; Schneider, M. D. Cardiac muscle regeneration: lessons from development. *Genes Dev.* **2011**, *25* (4), 299−309.

(5) Noseda, M.; Peterkin, T.; Simões, F. C.; Patient, R.; Schneider, M. D. Cardiopoietic factors: Extracellular signals for cardiac lineage commitment. *Circ. Res.* **2011**, *108*, 129−152.

(6) Willems, E.; Spiering, S.; Davidovics, H.; Lanier, M.; Xia, Z.; Dawson, M.; Cashman, J.; Mercola, M. Small molecule inhibitors of the Wnt pathway potently promote cardiogenesis in human embryonic stem cell-derived mesoderm. *Circ. Res.* **2011**, *109*, 360−364.

(7) Chen, B.; Dodge, M. E.; Tang, W.; Lu, J.; Ma, Z.; Fan, C. W.; Wei, S.; Hao, W.; Kilgore, J.; Williams, N. S.; Roth, M. G.; Amatruda, J. F.; Chen, C.; Lum, L. Small molecule-mediated disruption of Wnt-dependent signaling in tissue regeneration and cancer. *Nat. Chem. Biol.* **2009**, *5* (2), 100−107.

(8) Lu, J.; Ma, Z.; Hsieh, J. C.; Fan, C. W.; Chen, B.; Longgood, J. C.; Williams, N. S.; Amatruda, J. F.; Lum, L.; Chen, C. Structure-activity relationship studies of small-molecule inhibitors of Wnt response. *Bioorg. Med. Chem. Lett.* **2009**, *19* (14), 3825−3827.

(9) Luu, H. H.; Zhang, R.; Haydon, R. C.; Rayburn, E.; Kang, Q.; Si, W.; Park, J. K.; Wang, H.; Peng, Y.; Jiang, W.; He, T. C. Wnt/beta-catenin signaling pathway as a novel cancer drug target. *Curr. Cancer Drug Targets* **2004**, *4* (8), 653−671.

(10) Tian, Y.; Cohen, E. D.; Morrisey, E. E. The importance of Wnt signaling in cardiovascular development. *Pediatr. Cardiol.* **2010**, *31* (3), 342−348.

(11) Schneider, V. A.; Mercola, M. Wnt antagonism initiates cardiogenesis in *Xenopus laevis*. *Genes Dev.* **2001**, *15* (3), 304−315.

(12) Marvin, M. J.; Di Rocco, G.; Gardiner, A.; Bush, S. M.; Lassar, A. B. Inhibition of Wnt activity induces heart formation from posterior mesoderm. *Genes Dev.* **2001**, *15* (3), 316−27.

(13) Yang, L.; Soonpaa, M. H.; Adler, E. D.; Roepke, T. K.; Kattman, S. J.; Kennedy, M.; Henckaerts, E.; Bonham, K.; Abbott, G. W.; Linden, R. M.; Field, L. J.; Keller, G. M. Human cardiovascular progenitor cells develop from a KDR+ embryonic-stem-cell-derived population. *Nature* **2008**, *453* (7194), 524−528.

(14) Huang, S. M.; Mishina, Y. M.; Liu, S.; Cheung, A.; Stegmeier, F.; Michaud, G. A.; Charlat, O.; Wiellette, E.; Zhang, Y.; Wiessner, S.; Hild, M.; Shi, X.; Wilson, C. J.; Mickanin, C.; Myer, V.; Fazal, A.; Tomlinson, R.; Serluca, F.; Shao, W.; Cheng, H.; Shultz, M.; Rau, C.; Schirle, M.; Schlegl, J.; Ghidelli, S.; Fawell, S.; Lu, C.; Curtis, D.; Kirschner, M. W.; Lengauer, C.; Finan, P. M.; Tallarico, J. A.; Bouwmeester, T.; Porter, J. A.; Bauer, A.; Cong, F. Tankyrase inhibition stabilizes axin and antagonizes Wnt signalling. *Nature* **2009**, *461* (7264), 614−620.

(15) Gonsalves, F. C.; Klein, K.; Carson, B. B.; Katz, S.; Ekas, L. A.; Evans, S.; Nagourney, R.; Cardozo, T.; Brown, A. M.; DasGupta, R. An RNAi-based chemical genetic screen identifies three small-molecule inhibitors of the Wnt/wingless signaling pathway. *Proc. Natl. Acad. Sci. U.S.A.* **2011**, *108* (15), 5954−5963.

(16) Saraswati, S.; Alfaro, M. P.; Thorne, C. A.; Atkinson, J.; Lee, E.; Young, P. P. Pyrvinium, a potent small molecule Wnt inhibitor, promotes wound repair and post-MI cardiac remodeling. *PLoS One* **2011**, *5* (11), No. e15521.

(17) Wang, H.; Hao, J.; Hong, C. C. Cardiac induction of embryonic stem cells by a small molecule inhibitor of Wnt/beta-catenin signaling. *ACS Chem. Biol.* **2011**, *6* (2), 192−197.

(18) Letamendia, A.; Labbe, E.; Attisano, L. Transcriptional regulation by Smads: crosstalk between the TGF-beta and Wnt pathways. *J. Bone Joint Surg. Am.* **2001**, *83-A* (Suppl 1, Pt 1), S31−39.

(19) Lim, J. Y.; Kim, W. H.; Kim, J.; Park, S. I. Involvement of TGF-beta1 signaling in cardiomyocyte differentiation from P19CL6 cells. *Mol. Cells* **2007**, *24* (3), 431−436.

(20) Kattman, S. J.; Witty, A. D.; Gagliardi, M.; Dubois, N. C.; Niapour, M.; Hotta, A.; Ellis, J.; Keller, G. Stage-specific optimization of activin/nodal and BMP signaling promotes cardiac differentiation of mouse and human pluripotent stem cell lines. *Cell Stem Cell* **2011**, *8* (2), 228−240.

(21) Gustafson, T. A.; Markham, B. E.; Morkin, E. Analysis of thyroid hormone effects on myosin heavy chain gene expression in cardiac and soleus muscles using a novel dot-blot mRNA assay. *Biochem. Biophys. Res. Commun.* **1985**, *130* (3), 1161−1167.

(22) Sprague, P. W.; Heikes, J. E.; Gougoutas, J. Z.; Malley, M. F.; Harris, D. N.; Greenberg, R. Synthesis and in vitro pharmacology of 7-oxabicyclo[2.2.1]heptane analogues of thromboxane A2/PGH2. *J. Med. Chem.* **1985**, *28* (11), 1580−1590.